Polymer Journal (2019) 51:1103–1116
https://doi.org/10.1038/s41428-019-0237-9

REVIEW

Bridged polysilsesquioxane membranes for water desalination

Kazuki Yamamoto[1] · Joji Ohshita[2]

Received: 11 April 2019 / Revised: 25 May 2019 / Accepted: 19 June 2019 / Published online: 19 July 2019

Abstract

Water desalination through a reverse osmosis (RO) membrane is an important technology for producing pure water from seawater. High-performance membrane materials have been extensively developed because these materials are useful as core elements in practical water separation processes. Bridged polysilsesquioxane (PSQ)-derived membranes are promising candidates for robust RO membranes because they exhibit high thermal stability and chlorine resistance compared to conventional aromatic polyamide membranes. This review reports on our recent studies involving the development of RO membranes based on bridged PSQs. Our goal is to attain high water permeance with high salt rejection by optimizing the bridged PSQ structure. We have found that the introduction of hydrophilic and/or rigid bridging units tends to enhance water permeability. The preparation and evaluation of bridged PSQ RO membranes for water desalination based on the effects of the bridge structures are described. The bridged PSQ membranes are typically prepared by using a sol–gel process that involves hydrolysis/condensation of bridged alkoxysilane precursors to form sols followed by coating of the resulting sols and calcination of the coated sols to afford the gel membranes. Because the sol–gel process is a complicated multistep process, the development of a new and simpler process has been pursued. Herein, we summarize the recently introduced interfacial polymerization approach as a new method to readily prepare bridged PSQ RO membranes.

Introduction

Membrane separation is an efficient and simple process for separating gas or liquid from mixtures with low energy consumption and has a variety of applications ranging from industrial processes to household use [1–4]. The separation membrane enables the selective permeation of a target molecule, and this approach has been adopted for practical use in various industrial chemical processes. For example, a gas separation membrane is used to remove carbon dioxide from natural gas as well as recover hydrogen from air. In addition, membrane separation is used for water purification. Water separation membranes are classified into several types based on pore size. Microfilters, ultrafilters, and nanofilters are used to remove suspended solids and bacteria, viruses, and relatively large ions, such as Ca^{2+}, respectively. A reverse osmosis (RO) membrane with a pore size of <1 nm can remove even small ions, such as Na^{+}, from various water sources for ultrapure water production in semiconductor processes, wastewater treatment, and seawater desalination to produce drinkable water. Conventional RO membranes have a thin separation layer that is prepared on a porous support substrate. An asymmetric structure consisting of multiple separation layers with different permeability and separation properties is also used for the preparation of RO membranes. Because the performance of the membranes primarily depends on the separation layer, much attention has been focused on the development of new materials for the separation layer. The permeation mechanism is based on molecular exclusion effects that depend on pore size and ion size differences as well as the affinity of the membrane surface and the inner pore wall to water and ions, which affects the solubility and diffusivity of ions in the membrane as well as the water permeability [5]. The first practical RO membrane that was developed in the 1960s was an asymmetric cellulose acetate membrane [6–8]. In the 1970s, aromatic polyamide (PA)-based thin film composite membranes that exhibited high water permeance and high salt rejection were

✉ Joji Ohshita
jo@hiroshima-u.ac.jp

[1] Department of Pure and Applied Chemistry, Faculty of Science and Technology, Tokyo University of Science, 2641 Yamazaki, Noda, Chiba 278-8510, Japan

[2] Department of Applied Chemistry, Graduate School of Engineering, Hiroshima University, 1-4-1 Kagamiyama, Higashi-Hiroshima 739-8527, Japan

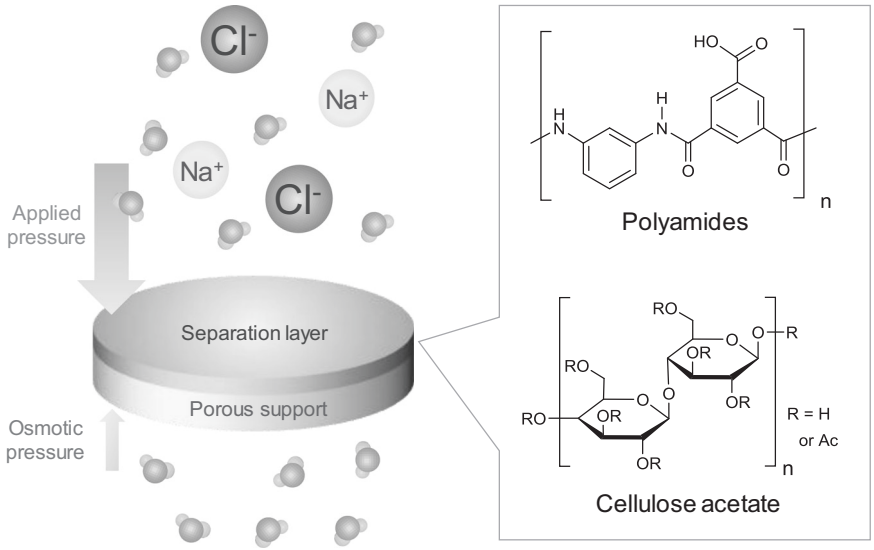

Fig. 1 Reverse osmosis membrane and commercially used materials

developed, and these membranes have continued to dominate the market (Fig. 1) [9–12]. However, the critical issue facing PA-based membranes is their chemical and thermal instability. In general, the permeability of water separation membranes is suppressed after long-term operation due to fouling of the separation layer surface by organic and/or inorganic substances. Although chlorine treatment is effective for removing fouling, the PA membrane is chlorine-labile due to cleavage of the amide bonds upon exposure to chlorine-based reagents [12, 13]. To overcome this issue, three approaches are available, including modification of the PA membrane surface (e.g., by polymer blushes to prevent foulant from contacting the surface) [14], development of chlorine-resistant materials by derivatization of the PA chemical structure [1], and composite (mixed matrix membrane) formation with inorganic fillers, such as silica [15], titania [16], metal organic framework [17], zeolite [18], and carbon nanotubes [19]. In addition, PA-based membranes are thermally unstable and can only be used at operation temperatures <45 °C [20, 21]. Therefore, new non-PA robust materials are highly desired for membrane stability improvement. Inorganic fillers are also employed to improve thermal stability [22, 23].

Polysilsesquioxanes (PSQs) with the general chemical formula $[RSiO_{1.5}]_n$ are typical organic–inorganic hybrid materials that can be obtained from the hydrolysis/condensation of trialkoxysilanes or trihalosilanes. The properties of PSQs are intermediate between those of silicone and silicate and derived from their unit structure (i.e., three Si-O bonds and one Si-R bond on one silicon atom). In general, PSQs exhibit high thermal, chemical, and mechanical stability due to their three-dimensional strong siloxane (Si-O-Si)-based framework. The organic group (R) is responsible for several functionalities, including

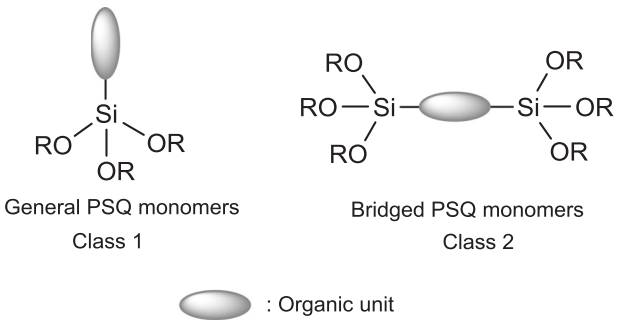

Fig. 2 Chemical structures of polysilsesquioxane monomers

flexibility, reactivity, and photoactivity, and a variety of applications, such as mechanical and thermal fillers, optical and electronic materials, and ceramic precursors [24–27]. Figure 2 shows two classes of PSQ monomers. Class 1 monomers have one reactive trialkoxysilane moiety. However, class 2 monomers bear two or more trialkoxysilane units. In the past few decades, bridged PSQs derived from class 2 monomers have received much attention due to their interesting properties (e.g., high porosity) that cannot be readily achieved using simple class 1 monomers (Fig. 3). PSQs based on class 2 monomers were first investigated by Lin et al. and Loy and Shea [28, 29]. Then Corriu et al. [30, 31] studied the polymerization behavior, appearance, and chemical structures of gels and demonstrated that the bridge structures of class 2 alkoxysilane monomers substantially affected the gel properties. To date, a variety of class 2 monomers have been subjected to the sol–gel process, and the applications of the resulting bridged PSQs as highly porous and low-density materials for use as adsorbents, catalysts, and heat insulators have been explored [32–36].

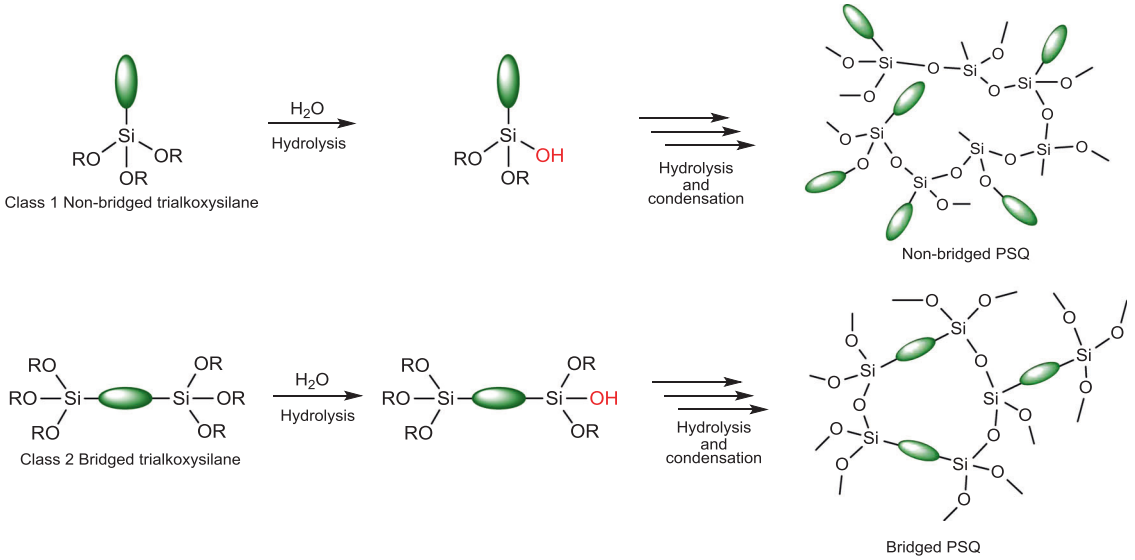

Fig. 3 Hydrolysis and condensation polymerization of class 1 and 2 alkoxysilanes to form non-bridged and bridged polysilsesquioxanes

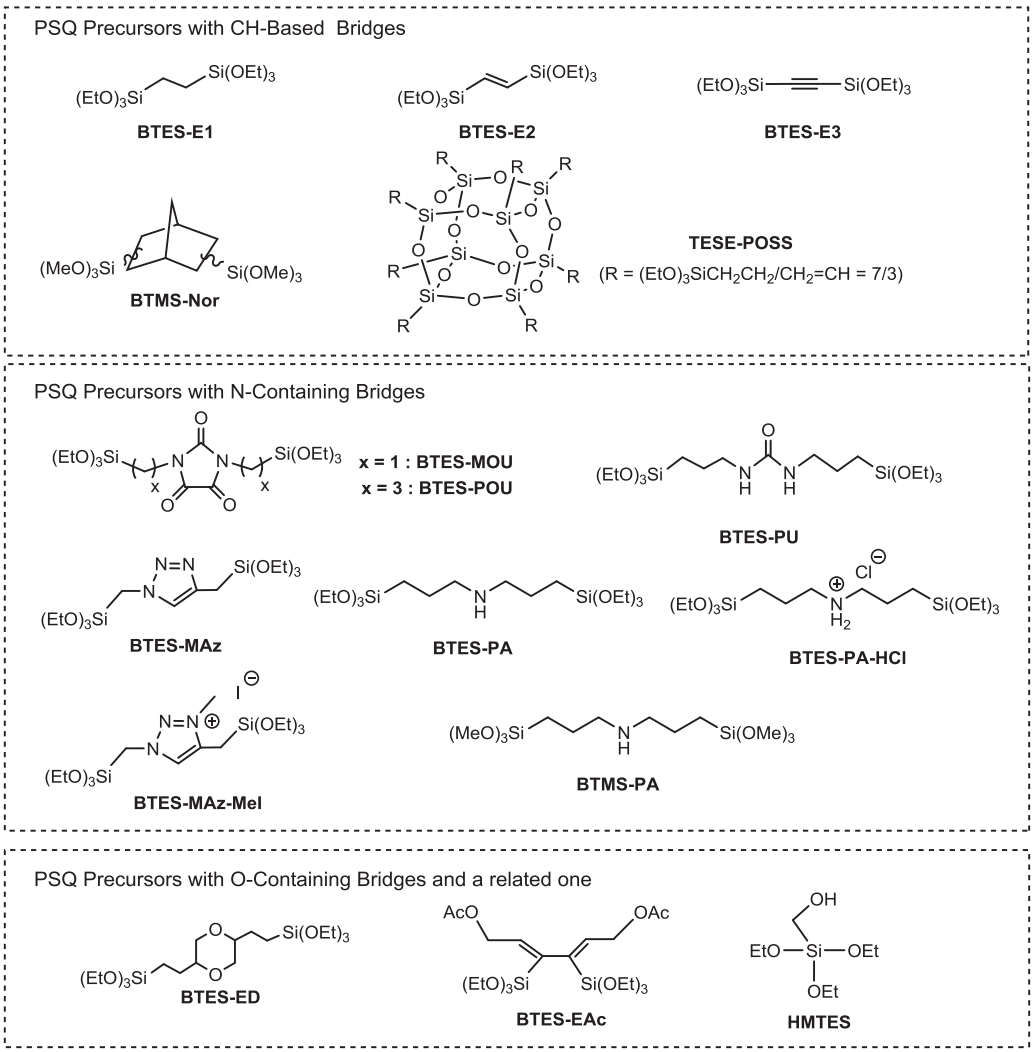

Fig. 4 Polysilsesquioxane precursors

Scheme 1 Synthesis of class 2 monomers

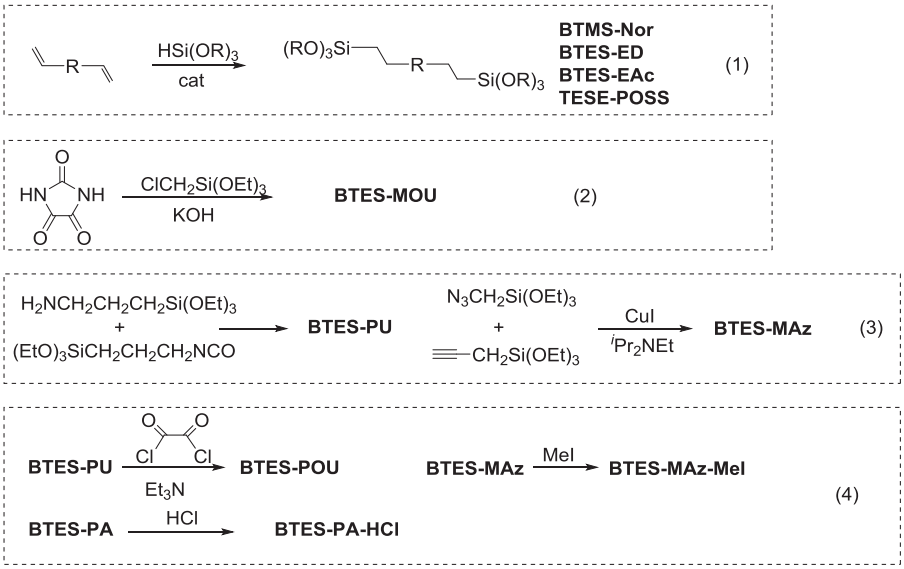

Table. 1 Properties and water separation performance of PSQ membranes

Entry	Monomer	Support	Calcination temp. [°C]/atmosphere	Water permeance [10^{-13} $m^3/(m^2 \cdot Pa \cdot s)$]	NaCl rejection [%]	Contact angle [°]	Pencil hardness	BET surface area [m^2/g]	Ref.
1	**BTES-E1**	Ceramic	300/N_2	1.0	98	66.8	>6H	522	[41]
2	**BTES-E2**	Ceramic	300/N_2	2.0	99	50.4	—	611	[42]
3	**BTES-E3**	Ceramic	300/N_2	8.5	95	48.4	—	763	[43]
4	**BTMS-Nor**	Ceramic	300/N_2	0.63	95	68.4	>6H	336	[54]
5	**BTES-MOU**	Ceramic	300/N_2	2.6	90	46.2	5H	155	[53]
6	**BTES-POU**	Ceramic	300/N_2	0.78	85	74.0	4B	0	[53]
7	**BTES-ED**	Ceramic	300/N_2	1.8	98.5	69.0	2H	373	[55]
8	**BTES-MAz**	Polymer	120/Air	3.7	96	69.0	2B	ND	[52]
9	**BTES-PA**	Polymer	150/Air	0.3	95	61.4	>6H	125	[51]
10	**BTES-PA-HCl**	Polymer	150/Air	0.24	97	57.3	>6H	ND	[51]
11	**HMTES**[a]	Ceramic	300/N_2	3.4	95.5	83.0	H	ND	[48]
12	**BTES-EAc**[a]	Ceramic	250/N_2	3.5	96	62.0	4H	ND	[49]
13	**TESE-POSS**	Ceramic	300/N_2	0.76	88	89	>6H	394	[50]
14	**TESE-POSS**[b]	Ceramic	300/N_2	1.4	86	82.0	>6H	424	[50]

BET Brunauer–Emmett–Teller, *ND* not determined, *PSQ* polysilsesquioxane

[a]Copolymer with **BTES-E1** (50 wt%). Water separation data improved with increasing RO operation time, and the data at the steady state are shown

[b]Copolymer with **BTES-E1** (80 wt%). Water separation data improved with increasing RO operation times, and the data at the steady state are shown

The bridged PSQ-based materials can also be employed for the fabrication of separation membranes. Castricum et al. prepared a copolymer consisting of bis(triethoxysilyl) ethane (**BTES-E1**) and methyltriethoxysilane as the first example of a separation membrane with a bridged PSQ-based separation layer and reported its application to *n*-butanol dehydration. Interestingly, this membrane exhibited high temperature durability at 90 °C under humid conditions in contrast to silica membrane [37, 38]. The durability was due to the stability of the Si-C bonds in the PSQ network toward hydrolysis, increasing the hydrothermal stability of the membrane. Kanezashi, Tsuru, and coworkers reported that a bridged PSQ prepared by homopolymerization of **BTES-E1** exhibited enhanced porosity, resulting in increased membrane gas permeance compared to the corresponding non-bridged PSQ membrane

prepared from a typical class 1 monomer (i.e., methyltriethoxysilane) [39, 40]. **BTES-E1**-derived membranes can be used as RO membranes for water desalination with high thermal stability and chlorine resistance, indicating the high potential of bridged PSQs as robust RO membrane materials [41]. In addition, ethenylene and ethynylene were introduced as C2 spacers in place of ethylene in **BTES-E1** to further improve the porosity, enhancing water permeability [42, 43]. This result clearly suggests that the bridge structure plays an important role in tuning separation properties. Similar bridged PSQ-based membranes have also been studied for other separation applications, such as gas separation [44–47].

Although these bridged PSQ membranes exhibit robust properties, water permeance is inferior to that of conventional PA membranes. Therefore, our research group has investigated the preparation of bridged silsesquioxane membranes from various class 2 monomers for the past decade with the aim of increasing water permeability without losing selectivity (i.e., salt rejection for water desalination). Herein, we provide a review of our research efforts for the preparation and evaluation of bridged PSQ-based RO membranes for water desalination and discuss how the bridge structures affect membrane performance. In addition, we describe our recent work on interfacial polymerization, a new membrane preparation method.

Class 2 bridged PSQ monomers

Various class 2 bridged trialkoxysilane monomers have been subjected to the sol–gel process to prepare RO membranes. As previously mentioned, Kanezashi, Tsuru, and coworkers reported that bridged PSQ membranes prepared from ethylene- and ethenylene-bridged monomers (**BTES-E1** and **BTES-E2**) exhibited RO properties with high thermal stability and chlorine resistance [41]. Through our collaborations with this group, we developed ethynylene-bridged monomer **BTES-E3** [43]. Membrane water permeance increases with increasing unsaturation number of the monomer C2 bridge in the following order: **BTES-E1<BTES-E2<BTES-E3**. However, salt rejection was decreased slightly in the same order. The introduction of a rigid bridge may increase the pore size as the small ring formation would be suppressed by the rigidity. In addition, the polar π–electron systems in **BTES-E2** and **BTES-E3** may enhance the membrane hydrophilicity.

In general, the membrane performance for water desalination can be evaluated based on two parameters: water permeability and NaCl rejection. However, these parameters are typically in a trade-off relationship, and the introduction of a finely designed bridging unit is necessary to improve both parameters. To optimize the monomer structure to prepare a high-performance desalination RO membrane, we have examined a variety of bridges with different rigidities and hydrophilicities, as shown in Fig. 4, to tune the resulting membrane porosity and water affinity, respectively. The bridging units are composed of a core unit and spacers that link the core and the reactive

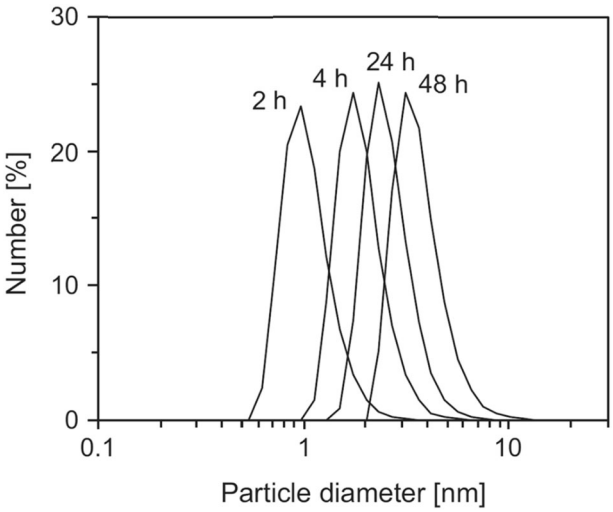

Fig. 5 Preparation of **BTES-MAz** sol with size control at various string times at room temperature. Reproduced with permission from [52]

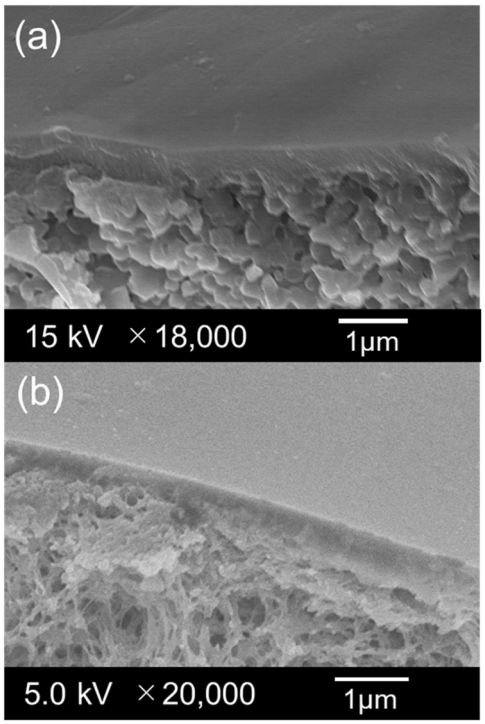

Fig. 6 Cross-sectional scanning electron microscopic images of membranes prepared from **a HMTES** on a ceramic support and **b BTES-MAz** on an organic polymer support. Reproduced with permission from [48, 52]

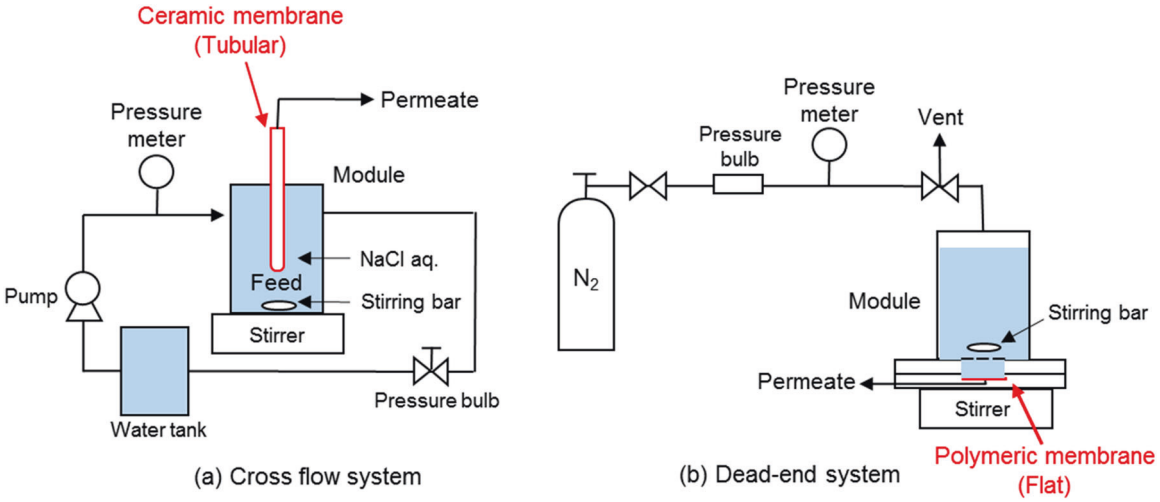

Fig. 7 Evaluation of reverse osmosis membrane performance using an **a** inorganic tubular support and **b** organic flat support

trialkoxysilane units unless the silicon units can be directly introduced onto the core unit. Class 2 monomers are obtained from commercial sources, synthesized according to the literature procedures, or newly synthesized by hydrosilylation (1), nucleophilic substitution (2), construction of the core unit (3), or modification of the core unit (4), as shown in Scheme 1.

Copolymerization for membrane preparation was also investigated to finely tune PSQ properties to improve membrane performance. For example, **BTES-E1** was copolymerized with other monomers, including a non-bridged highly hydrophilic trialkoxysilane (**HMTES**) [48], acetoxy-containing monomer (**BTES-EAc**) [49], or cage-type silsesquioxane-based monomer (**TESE-POSS**) [50] using several monomer ratios (Table 1, Entries 11−14).

Sol–gel process and bulk gel properties

The RO membranes were prepared using a sol–gel process that involved hydrolysis/polymerization of the monomers under mild conditions to form sols followed by coating of the sols on inorganic supports and calcination to induce gel formation. Under standard conditions, a mixture of reagent and reactant in an HCl/monomer/H_2O molar ratio of 0.1/1/60 with 5 wt% monomer concentration in ethanol was gently stirred at room temperature for 2 h, except for **BTES-PA** [51], **BTMS-PA** [51], **BTES-MAz** [52], and **BTES-MAz-MeI** [52]. The **BTES-PA**, **BTMS-PA**, **BTES-MAz**, and **BTES-MAz-MeI** monomers were polymerized in the absence of HCl because the amine unit catalyzed the hydrolysis/condensation as a self-catalyst. In this process, control of the sol particle size was important. The sol particle diameter should be larger than the pore size to avoid permeation of the sols into the pore, but the use of sols that are too large must be avoided to form dense and homogeneous membranes. The sol particle diameter can be primarily controlled by the reaction time, and a large amount of water should be used if the reactions are proceeding too slowly to complete the formation of suitably sized sols within a reasonable stirring period. Sol particle diameters were estimated by dynamic light scattering, and the reactions were continued until the sol particle diameters were 2–10 nm, which were suitable for coating on a porous substrate with a pore size of approximately 1–2 nm. Figure 5 shows an example of sol size control for **BTES-MAz** upon hydrolysis with water in ethanol. Stirring a 5 wt% ethanol solution consisting of **BTES-MAz** with 60 eq. of water at room temperature led to a gradual increase in the sol size that exceeded 2 nm after 24 h. This material was suitable for coating on a porous substrate. Then the sol films that were coated on the porous support were calcined to yield gel membranes. In addition, the calcination temperature must be carefully adjusted. High-temperature calcination would facilitate condensation, resulting in the formation of dense membranes. However, heating at a temperature that is too high would cause thermal decomposition of the organic bridging units. Therefore, the calcination temperatures were carefully determined based on thermogravimetric analysis (TGA) and temperature-dependent infrared (IR) spectrometry of the polymers. For example, the **BTES-MOU** and **BTES-POU** membranes were prepared by calcination of the sol films at 300 °C in a nitrogen atmosphere because no significant weight loss (2–4%) was observed during the TGA up to this temperature. In addition, nearly the same IR spectra were obtained after heating at 300 °C, except that the signal intensities of the silanol bonds decreased and those of the siloxane units increased [53]. However, at 400 °C, the weight loss reached 10–20%, and the IR signals due to organic groups including the signals corresponding to C-H bonds were considerably weakened.

We used two types of porous supports in our studies. The inorganic supports were composed of layered ceramic substrates with the following structure: SiO_2-ZrO_2/TiO_2/Al_2O_3. The organic supports were composed of a sulfonated polysulfone skin layer on polysulfone/polyethylene terephthalate unwoven cloth. The inorganic supports permitted calcination at a high temperature to enhance membrane network structure and porosity. However, the organic supports were typically thermally less stable, and the currently used organic supports readily underwent thermal decomposition at temperatures >150 °C. However, flexible RO membranes could be prepared using organic supports rather than inorganic rigid supports. Furthermore, the currently studied organic supports are commercially available and easy to handle. The prepared membranes were analyzed by performing scanning electron microscope (SEM) measurements to examine the thickness, morphology, and conditions of the membranes, as illustrated in Fig. 6. Only the membranes that exhibited no defects, such as cracks and pinholes, in the SEM images of the surfaces were subjected to subsequent RO experiments. In addition, the water contact angles of the membrane surface and nitrogen adsorption/desorption isotherms were measured to determine porosity and the Brunauer–Emmett–Teller (BET) surface areas of the gels prepared by drying the sols as well as the membrane hydrophilicity, respectively.

Water desalination performance

Evaluation of RO performance

Figure 7 shows the apparatus setting for the RO experiments of the membranes prepared on inorganic ceramic supports and organic polymer supports. The experiments were performed using a 2000-ppm NaCl aqueous solution by applying a feed pressure of 1.0 MPa at 25 °C. As important parameters for the evaluation of membrane performance, the water permeance (L_p) and NaCl rejection (R) of the bridged PSQ membranes obtained from the RO experiments are summarized in Table 1. These values were determined based on the following equations: $L_p = J_v/(\Delta P - \Delta\pi)$ and $R = (1 - C_p/C_f)$, respectively, where J_v, ΔP, and $\Delta\pi$ are the water volume flux, difference in applied pressure, and difference in osmotic pressure, and C_p and C_f are the NaCl concentrations of the permeate and feed, respectively. Some membranes exhibited an increase in water permeance and NaCl rejection at an early stage in each RO experiment, and the data collected after several hours at the experimental steady state are listed in Table 1. The increase in water permeance and NaCl rejection in the early stage of the experiments may be due to the duration required to wet the membrane surface and the inner pore wall during water immersion as well as the electrostatic repulsion resulting from adsorption of NaCl ions to the membranes, respectively.

PSQ membranes with hydrocarbon bridges

A comparison of membranes prepared from simple C2-bridged monomers indicated that those from **BTES-E2** and **BTES-E3** with rigid ethenylene and ethynylene bridges possessed higher water permeability than the membrane obtained from **BTES-E1** with a flexible ethylene bridge even though the NaCl rejection decreased slightly, as previously mentioned [41–43]. The bridge rigidity of **BTES-E2** and

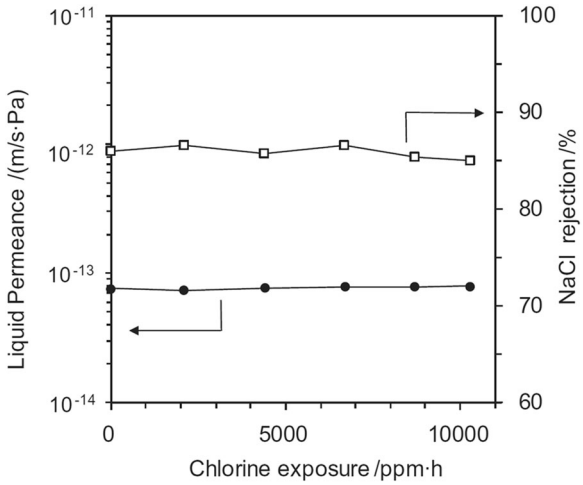

Fig. 8 Effects of chlorine exposure on liquid permeance and NaCl rejection of **TESE-POSS** membranes using a 100 ppm NaOCl solution. Reproduced with permission from [50]

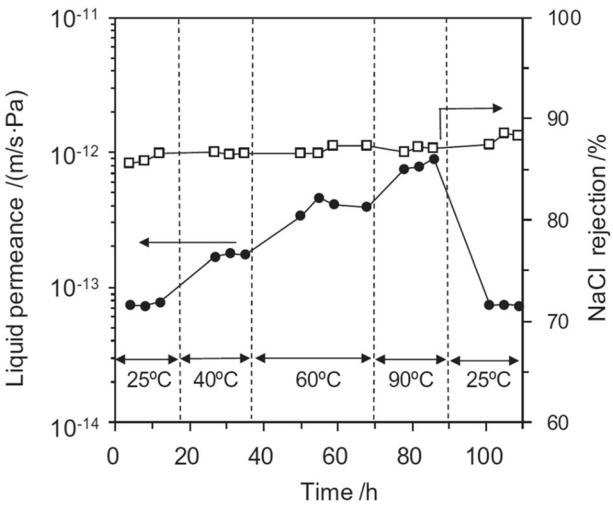

Fig. 9 Liquid permeance and NaCl rejection of **TESE-POSS** membranes as a function of the operation time using a 2000-ppm NaCl solution at 25–90 °C. Reproduced with permission from [50]

BTES-E3 most likely increased the tendency to form a sparse network due to the sterically fixed silicon reactive centers, enhancing the membrane porosity. This result is in contrast to that with **BTES-E1**, which possessed a flexible ethylene unit that would allow changes in the relative positions of the silicon centers and the potential to form a denser network. In fact, the BET surface areas of the gels prepared from **BTES-E1**, **BTES-E2**, and **BTES-E3**, which were determined by nitrogen adsorption/desorption experiments, increased in this order (Table 1, Entries 1−3). Increasing the number of C-H bonds in the bridges would sterically hinder water permeability in the following order: **BTES-E3<BTES-E2<BTES-E1**. In addition, the introduction of polar π–electron systems would improve membrane water affinity, as indicated by the decreased water contact angles on the membrane surface (Table 1, Entries 1−3). These results inspired us to introduce highly rigid norbornanediyl as the bridging unit (**BTES-Nor**) [54]. As expected, a porous membrane was obtained by subjecting **BTES-Nor** to the sol–gel process (Table 1, Entry 4). However, its water permeance was lower than those of the C2-bridged membranes, which was most likely due to its higher hydrophobicity.

We also examined POSS (polyhedral oligomeric silsesquioxane)-based monomer **TESE-POSS** because the rigid cubic structure of POSS might provide intercubic pores to enhance membrane porosity [50]. As expected, the **TESE-POSS** homopolymer gel exhibited moderate porosity with a surface area of 394 m^2/g. However, its water separation RO properties were inferior to those of the membranes prepared from **BTES-E1**, **BTES-E2**, and **BTES-E3** with C2 bridges. The copolymerization of **TESE-POSS** with **BTES-E1** enhanced the porosity and improved the RO performance. However, the performance was still lower than those of the C2-bridged membranes. The POSS-containing membranes are most likely too hydrophobic to exhibit good water permeability with moderate NaCl rejection, which was observed for the **BTES-Nor**-based membrane. However, it is important to note that these membranes that contain hydrocarbon bridges exhibit high thermal stability, high mechanical strength, and high chlorine resistance. Therefore, these membranes are useful as robust membranes for water desalination. For example, **TESE-POSS**-based membranes exhibited a pencil harness >6H and underwent no evident changes in performance even after treatment with hot water at 90 °C for 20 h or exposure to chlorine-containing water up to 10,000 ppm·h, as shown in Figs. 8 and 9. This result is in contrast to that observed for a typical PA membrane that must be used <45 °C [20]. A decrease in permeability by long-term operation at 65 °C has been reported, which may be due to compaction of the swelled PA film [21]. In addition, a commercial PA membrane loses its salt-rejection properties after approximately 10,000 ppm·h chlorine exposure [12, 13].

PSQ membranes with amine-based polar units

We introduced oxalylurea to the monomers as a rigid polar bridging fragment. Owing to synthetic requirements, the oxalylurea core unit was linked to the reactive alkoxysilane centers by C1 and C3 linkers in **BTES-MOU** and **BTES-POU**, respectively [53]. Interestingly, the length of the linkers (C1 or C3) affected the porosity of the gels, and the membrane prepared from **BTES-MOU** was porous but **BTES-POU** resulted in a nonporous membrane due to C3 flexibility (Table 1, Entries 5, 6). Both the **BTES-MOU**- and **BTES-POU**-derived membranes exhibited water separation properties in RO experiments, which are most likely due to molecular sieving effects and a diffusion-controlled mechanism for the membranes prepared from **BTES-MOU** and **BTES-POU**, respectively. However, the **BTES-MOU**-derived membrane exhibited higher water permeance and higher NaCl rejection than the **BTES-POU**-derived membrane, suggesting that the introduction of a rigid polar bridge is preferable for the preparation of high-performance RO membranes for water separation. A monomer containing a polar urea core unit (**BTES-PU**) was also examined for membrane preparation. However, the resulting membrane exhibited RO properties inferior to those of the **BTES-POU** membrane, which may be due to urea flexibility.

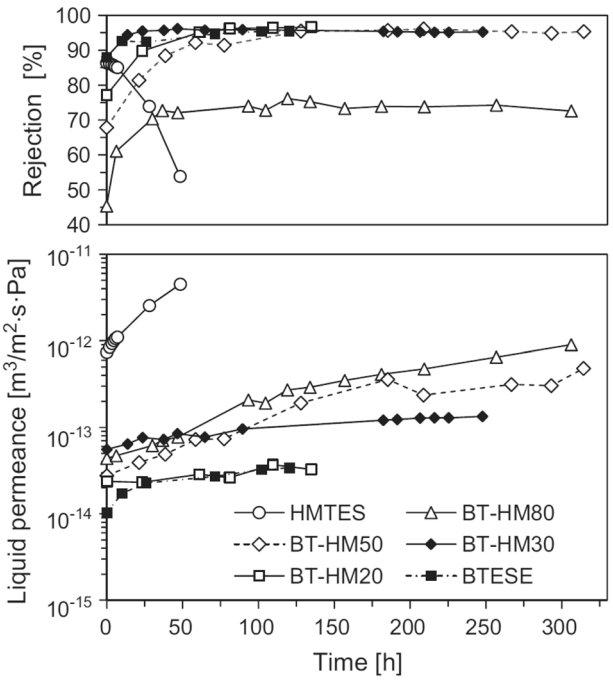

Fig. 10 Liquid permeance and NaCl rejection of homopolymer and copolymer membranes of **HMTES** and **BTES-E1** as a function of operation time of the reverse osmosis experiment using a 2000-ppm NaCl solution. Numbers in abbreviations indicate wt% values of **HMTES** loaded for copolymerization. Reproduced with permission from [48]

As a rigid polar spacer, we also prepared triazole-containing monomer **BTES-MAz**, as shown in Scheme 1 [52]. Unexpectedly, the **BTES-MAz**-derived membrane was less hydrophilic than the **BTES-E1**-based membrane based on the larger water contact angle on the **BTES-MAz**-based membrane surface (Table 1, Entries 1, 8). However, despite the relatively low hydrophilicity, the **BTES-MAz**-based membrane exhibited good performance that was comparable to that of the **BTES-E1**-based membrane. Interestingly, the membrane was softer than the membranes containing hydrocarbon spacers (pencil hardness = 2B). The flexibility of the **BTES-MAz**-based membrane appears to be advantageous for processability, especially when it is applied as a flexible membrane. We also examined ammonium-containing **BTES-MAz-MeI** as a monomer. As expected, the **BTES-MAz-MeI**-based membrane prepared from the sol–gel process exhibited a smaller water contact angle than the **BTES-MAz**-based membrane. However, the **BTES-MAz-MeI**-based membrane exhibited no salt separation properties, which was most likely due to the difficulty in controlling the sol particle size. In this case, the sol particle size easily exceeded 5 nm even after a short period of hydrolysis/condensation of **BTES-MAz-MeI**, which may be due to the higher water affinity of **BTES-MeI**. However, we have no direct data to help us understand the high reactivity of **BTES-MAz-MeI** toward hydrolysis/condensation.

To improve hydrophilicity, we investigated a secondary amine bridge with an active N-H bond (**BTES-PA**) [51]. **BTES-PA** was subjected to the sol–gel process, resulting in the formation of a porous membrane despite the high flexibility of the dipropyleneamine bridge. Interbridge hydrogen bonding is likely responsible for the formation of the porous membrane, which restricts bridge movement. The membrane exhibited good RO performance with moderate water permeability. The high hydrophilicity of the membrane, which is based on the relatively small water contact angle, would be one reason for the moderate water permeability. We also prepared membranes from ammonium-containing **BTES-PA-HCl** under several conditions. However, its membrane performance was comparable to that of **BTES-PA**-based membranes (Table 1, Entries 9, 10). No significant influence from ammonium formation on membrane performance was observed.

PSQ membranes with ether-, ester-, and hydroxyl-containing polar units

Dioxane-based monomer **BTES-ED** [55] and ester-containing precursor **BTES-EAc** [49] were prepared by

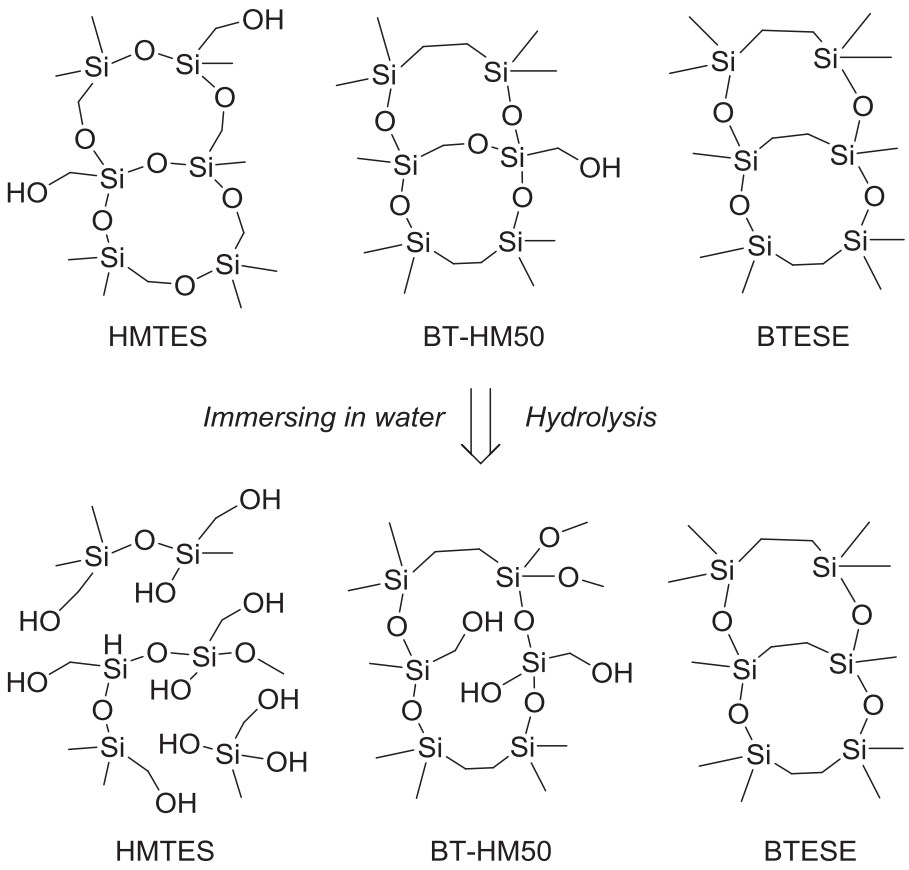

Scheme 2 Dehydrocoupling between alcohol and silanol. Reproduced with permission from [48]

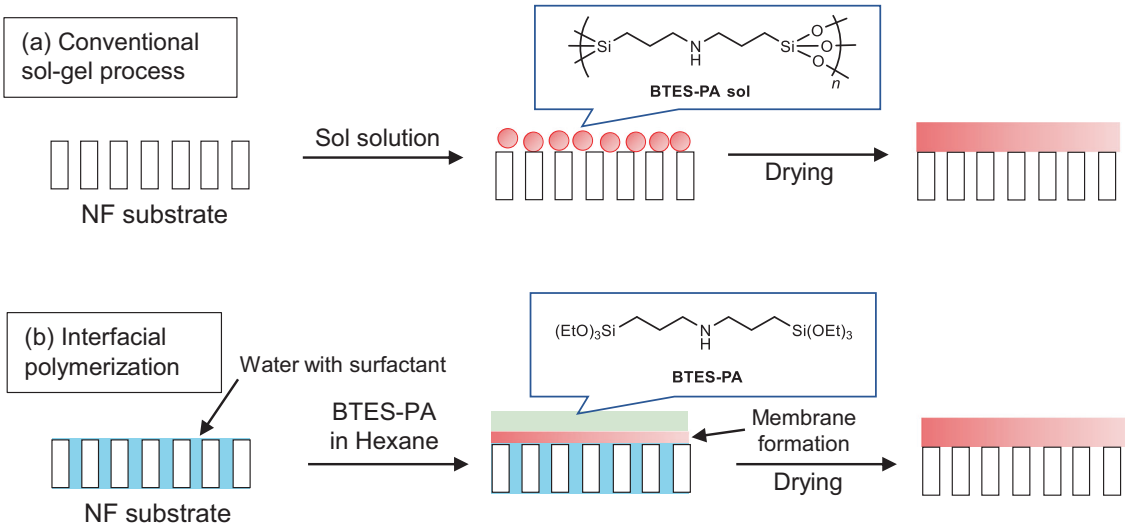

Fig. 11 Membrane preparation using this method

Pt-catalyzed hydrosilylation (Scheme 1). Monomer **BTES-ED** could also be converted to RO membranes using the sol–gel process, and the resulting membrane exhibited water separation properties that are comparable to those of **BTES-E2** and **BTES-E3** (Table 1, Entries 2, 3, 7). However, its water permeability was still unsatisfactory, and we introduced hydroxyl groups to the membranes by employing hydroxymethyltriethoxysilane (**HMTES**) as the monomer to further improve the membrane hydrophilicity [48]. Homopolymerization of **HMTES** with the sol–gel process provided a membrane that exhibited a water permeance of 7.3×10^{-13} $m^3/(m^2 \cdot s \cdot Pa)$ during the initial stage of the RO experiment. Although this value was as high as that of **BTES-E3**, the membrane underwent degradation, increasing water permeance during the RO experiment to approximately 5×10^{-13} $m^3/(m^2 \cdot s \cdot Pa)$ after 5 h of operation. At the same time, NaCl rejection of the **HMTES** homopolymer membrane decreased from 86% to 54%, and finally, the skin layer detached from the support (Fig. 10), which was likely due to hydrolysis of the C-O-Si bonds that had been formed by the dehydrocoupling between alcohol and silanol upon calcination, as shown in Scheme 2. The hydrolytic cleavage of the C-O-Si bonds was confirmed by comparing the IR spectra of the membrane before and after soaking in water. To improve the hydrolytic stability, **HMTES** was copolymerized with **BTES-E1** to increase the number of Si-O-Si bonds that were essentially nonreactive under the RO experiment conditions. As expected, the copolymer membranes exhibited improved stability. The water permeance increased as the operation time increased during the RO experiments until a steady state was reached. This result may be due to the hydrolysis of the C-O-Si bonds. However, unlike the **HMTES** homopolymer membrane, the process proceeded without suppressing NaCl

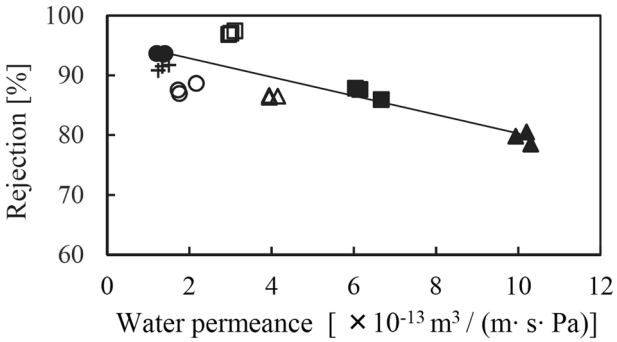

Fig. 12 Trade-off plots of water permeance and NaCl rejection of membrane. The line is a guide for the trade-off relationship of the **BTESPA** membrane prepared by interfacial polymerization (black circle (●): 5 wt% **BTESPA** 0.03 wt% sodium dodecyl sulfate (SDS), black square (■): 5 wt% **BTESPA** 0.15 wt% SDS, black triangle (▲): 1 wt% **BTESPA** 0.03 wt% SDS, white circle (○): 5 wt% **BTMSPA** 0.03 wt% SDS, white square (□): 1 wt% **BTMSPA** 0.03 wt% SDS, white triangle (△): 5 wt% **BTMSPA** 0.15 wt% SDS, and plus symbol (+): 5 wt% **BTESPA**, sol–gel process). Reproduced with permission from [57]

rejection when the **BTES-E1/HMTES** monomer ratio was ≥1. The best performance was observed for the copolymer membrane with a **BTES-E1/HMTES** monomer ratio of 1. These results indicate that posthydrolysis of the C-O-Si bonds after membrane preparation is an efficient method for controlling membrane hydrophilicity. In fact, no obvious changes in the RO performance were observed for the **BTES-E1** homopolymer membrane that lacked C-O-Si bonds. A membrane with an even higher water permeance was obtained using **BTES-E2** as the comonomer rather than **BTES-E1** even though the NaCl rejection decreased slightly [56]. Similar posthydrolysis was observed for the **BTES-EAc**-derived membranes. In these membranes, hydrolysis of the C-O-Si bonds formed via a side reaction

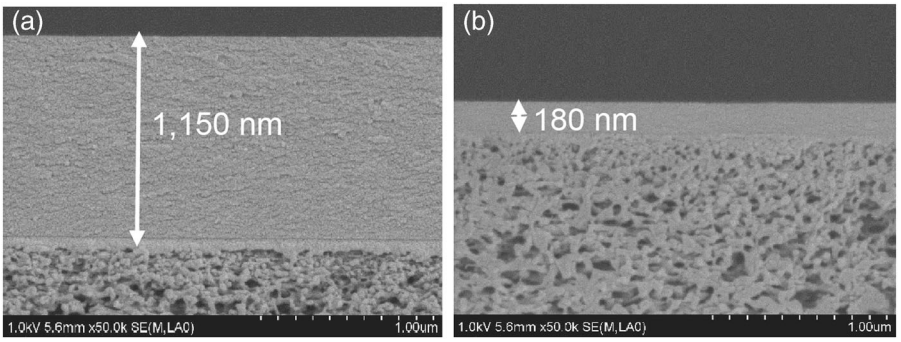

Fig. 13 Cross-sectional scanning electron microscopic images of membranes prepared from 5 wt% (**a**) and 1 wt% **BTESPA** (**b**) with 0.03 wt% sodium dodecyl sulfate. Reproduced with permission from [57]

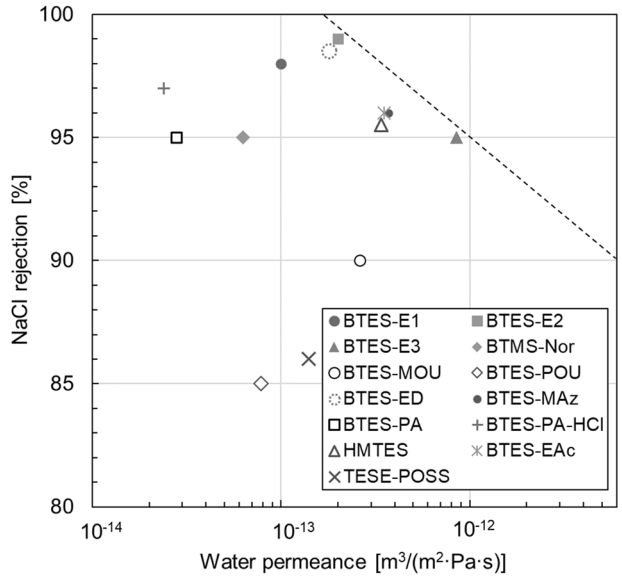

Fig. 14 Water separation performance of polysilsesquioxane membrane

during the sol–gel process must have occurred. Water permeance of the homopolymer membrane increased gradually during the RO experiment. However, its NaCl rejection increased and then decreased after exceeding the maximum value. In contrast, a similar experiment with a copolymer membrane prepared from **BTES-EAc** and **BTES-E1** exhibited only an increased water permeance without a decrease in the NaCl rejection prior to reaching a steady state after 120 h of operation.

Interfacial polymerization

The conventional sol–gel process is commonly utilized for the preparation of PSQ membranes due to its high reproducibility for separation layer preparation. However, the entire process including sol formation, coating, and calcination of the coated sol for conversion into a gel is complicated and requires careful control of the conditions for sol formation and calcination, as mentioned above. Therefore, the development of a new and simpler process is desired. Aromatic PA membranes are commercially prepared via the interfacial polymerization of tricarbonyl trichloride in organic solvent and diamine in water because polymerization is an easily controllable and cost-efficient process [1]. As a result, we adopted interfacial polymerization for the preparation of bridged PSQ membranes [57]. Figure 11 shows a schematic representation of interfacial polymerization for the formation of bridged PSQ membranes. In this process, a single monomer in organic solvent reacts with water at the interface. This process is in contrast to that in PA formation, which requires two monomers (i.e., one in an organic layer and the other in an aqueous layer). First, we employed **BTES-PA** as the monomer due to its relatively high solubility in water. Because the basic amine group in **BTES-PA** can catalyze the sol–gel polymerization and no additional catalyst is required, the reaction conditions were more easily tuned.

A porous polymer support was immersed in an aqueous solution containing a surfactant to improve monomer solubility in water. The excess aqueous solution was removed, and then a hexane solution containing **BTES-PA** was poured onto the support. After a while, the excess hexane solution was removed, and the resulting PSQ-coated support was calcined at 150 °C for 10 min to yield a separation membrane. Optimization of the reaction conditions by tuning the concentrations of the monomer and the surfactant as well as the reaction time led to the best trade-off (Fig. 12) between the water permeance (1.41×10^{-13} $m^3/(m^2 \cdot s \cdot Pa)$) and NaCl rejection (93.6%), which was superior to that prepared by the sol–gel process with **BTES-PA** (vide supra). It is important to note that the film thickness can be readily controlled by changing the monomer concentration, which exerts a significant influence on the water permeance and NaCl rejection of the membrane relative to the trade-off line for water permeance and NaCl rejection, as shown in Fig. 13. The membranes prepared using methoxysilane **BTMS-PA** as the monomer exhibited an even more favorable RO performance than the

ethoxysilane **BTES-PA**-derived membrane (i.e., water permeance of 3.11×10^{-13} $m^3/(m^2 \cdot s \cdot Pa)$ and NaCl rejection of 97.4%). However, **BTMS-PA** is much more reactive than **BTES-PA** because the methoxy groups in the former resulted in less steric hindrance than the ethoxy groups in the latter, making it more difficult to control the reaction progress in **BTMS-PA**. Less polar **BTES-E1** also underwent interfacial polymerization to provide RO membranes. However, in contrast to the membranes derived from **BTES-PA** and **BTMS-PA**, the **BTES-E1**-based membranes prepared by interfacial polymerization exhibited a much lower NaCl rejection than the **BTES-E1** membranes prepared by the sol–gel process. Therefore, the use of a polar monomer with an appropriate solubility in water is essential for preparing RO membranes with high NaCl rejection via interfacial polymerization.

Conclusions

We have prepared a variety of bridged PSQ membranes via hydrolysis/condensation of bridged alkoxysilane monomers and explored their utility as RO membranes for water desalination. Figure 14 shows the trade-off plots of water permeance and NaCl rejection of the bridged PSQ membranes, indicating the dependence of the performance on the bridge structures. Although the RO performance of the membranes is not sufficiently high compared to that of commercially available PA membranes, the robustness of the bridged PSQ membranes toward heat and chlorine exposure would be advantageous for practical use. By changing the rigidity and polarity of the bridges, we can control the porosity and hydrophilicity of the membranes, which directly affect membrane performance. However, further studies are necessary to fully understand the relationship between the monomer structure and the membrane performance to yield important insight into the structural design of the bridges.

The posthydrolysis of membranes prepared from the copolymerization of bridged PSQ precursors with **HMTES** offers a new methodology for tuning membrane hydrophilicity, thereby enhancing water permeability. Interfacial polymerization was examined as a simple, cost-efficient, and time-saving method for membrane preparation. It important to note that some of the bridged PSQ membranes were usable as gas separation membranes, including for CO_2 separation [53]. Further studies to improve the RO performance of the membranes and to explore other functionalities are currently underway.

Acknowledgements This research was supported by the "Development of Robust RO/NF Membranes for Various Types of Water Resources" project of the Core Research for Evolutional Science and Technology, Japan Science and Technology Agency (CREST, JST).

Compliance with ethical standards

Conflict of interest The authors declare that they have no conflict of interest.

Publisher's note: Springer Nature remains neutral with regard to jurisdictional claims in published maps and institutional affiliations.

References

1. Daer S, Kharraz J, Giwa A, Hasan SW. Recent applications of nanomaterials in water desalination: a critical review and future opportunities. Desalination 2015;367:37–48.
2. Padaki M, Sury R, Muralia M, Abdullaha S, Misdana N, Moslehyania A, et al. Membrane technology enhancement in oil–water separation. A review. Desalination 2015;357:197–207.
3. Bernardo P, Drioli E, Golemme G. Membrane gas separation: a review/state of the art. Ind Eng Chem Res 2009;48:4638–63.
4. Brunetti A, Scura F, Barbieri G, Drioli E. Membrane technologies for CO_2 separation. J Membr Sci 2010;359:115–25.
5. Mayyahi AA. Important approaches to enhance reverse osmosis (RO) Thin film composite (TFC) membranes performance. Membranes (Basel) 2018;8:E68.
6. Loeb S, Sourirajan S, US Patent US3133132A.
7. Idris A, Ismail AF, Noordin MY, Shilton SJ. Optimization of cellulose acetate hollow fiber reverse osmosis membrane production using Taguchi method. J Membr Sci 2002;205:223–37.
8. Duarte AP, Bordado JC, Cidade MT. Cellulose acetate reverse osmosis membranes: Optimization of preparation parameters. Appl Polym Sci 2007;103:134–9.
9. Karl A, Buder W, Eur. Pat. Appl., EP 50768 A2 1982.
10. Verbeke R, Gómez V, Vankelecom IFJ. Chlorine-resistance of reverse osmosis (RO) polyamide membranes. Prog Polym Sci 2017;72:1–15.
11. Kang GD, Gao CJ, Chen WD, Jie XM, Cao YM, Yuana Q. Study on hypochlorite degradation of aromatic polyamide reverse osmosis membrane. J Membr Sci 2007;300:165–71.
12. Shintani T, Matsuyama H, Kurata N. Development of a chlorine-resistant polyamide reverse osmosis membrane. Desalination 2007;207:340–8.
13. Park HB, Freeman BD, Zhang ZB, Snkir M, McGrath JE. Highly chlorine-tolerant polymers for desalination. Angew Chem Int Ed 2008;47:6019–24.
14. Kang GD, Cao YM. Development of antifouling reverse osmosis membranes for water treatment: a review. Water Res 2012;46:584–600.
15. Jadav GL, Singh PS. Synthesis of novel silica-polyamide nanocomposite membrane with enhanced properties. J Membr Sci 2009;328:257–67.
16. Safarpour M, Khataee A, Vatanpour V. Thin film nanocomposite reverse osmosis membrane modified by reduced graphene oxide/TiO_2 with improved desalination performance. J Membr Sci 2015;489:43–54.
17. Park HM, Jee KY, Lee YT. Preparation and characterization of a thin-film composite reverse osmosis membrane using a polysulfone membrane including metal-organic frameworks. J Membr Sci 2017;541:510–8.
18. Li L, Dong J, Nenoff TM, Lee R. Desalination by reverse osmosis using MFI zeolite membranes. J Membr Sci 2004;243:401–4.
19. Kim HJ, Baek Y, Choi K, Kim DG, Kang H, Choi YS, et al. The improvement of antibiofouling properties of a reverse osmosis membrane by oxidized CNTs. RSC Adv 2014;4:32802–10.

20. Li D, Wang H. Recent developments in reverse osmosis desalination membranes. J Mater Chem 2010;20:4551–66.
21. Khorshidi B, Biswas I, Ghosh T, Thundat T, Sadzadeh M. Robust fabrication of thin film polyamide-TiO_2 nanocomposite membranes with enhanced thermal stability and anti-biofouling propensity. Sci Rep 2018;8:784.
22. Duan J, Litwiller E, Pinnau I. Preparation and water desalination properties of POSS-polyamide nanocomposite reverse osmosis membranes. J Membr Sci 2015;473:157–64.
23. Saleh TA, Gupta VK. Synthesis and characterization of alumina nano-particles polyamide membrane with enhanced flux rejection performance. Sep Purif Technol 2012;89:245–51.
24. Baney RH, Itoh M, Sakakibara A, Suzuki T. Silsesquioxanes. Chem Rev 1995;95:1409–30.
25. Kim KM, Chujo Y. Organic-inorganic hybrid gels having functionalized silsesquioxanes. J Mater Chem 2003;13:1384–91.
26. Gunji T, Kaburagi H, Tsukada S, Yoshimoto A. Preparation, properties, and structure of polysiloxanes by acid-catalyzed controlled hydrolytic co-polycondensation of polymethyl(methoxy) siloxane and polymethoxysiloxane. J Sol-Gel Sci Technol 2015; 75:564–73.
27. Kaneko T. Ionic silsesquioxanes: preparation, structure control, characterization, and applications. Polymer 2018;144:205–24.
28. Lin DR, Hu LJ, Xing BS, You H, Loy DA. Mechanisms of competitive adsorption organic pollutants on hexylene-bridged polysilsesquioxane. Materials. 2015;8:5806–17.
29. Loy DA, Shea KJ. Bridged polysilsesquioxanes. Highly porous hybrid organic-inorganic materials. Chem Rev 1995;95:1431–42.
30. Corriu RJP, Moreau JJE, Thepot P, Man MWC. New mixed organic-inorganic polymers: hydrolysis and polycondensation of bis(trimethoxysilyl)organometallic precursors. Chem Mater 1992; 4:1217–24.
31. Corriu RJP, Moreau JJE, Thepot P, Man MWC. Hybrid silica gels containing 1,3-butadiyne bridging units. thermal and chemical reactivity of the organic fragment. Chem Mater 1996;8:100–6.
32. Brigo L, Faustini M, Pistore A, Kang HK, Ferraris C, Schutzmann S, et al. Porous inorganic thin films from bridged silsesquioxane sol–gel precursors. J Non-Cryst Solids 2016;432:399–405.
33. Yun S, Luo H, Gao Y. Low-density, hydrophobic, highly flexible ambient-pressure-dried monolithic bridged silsesquioxane aerogels. J Mater Chem A 2015;3:3390–8.
34. Zou F, Yue P, Zheng X, Tang D, Fu W, Li Z. Robust superhydrophobic thiourethane bridged polysilsesquioxane aerogels as potential thermal insulation materials. J Mater Chem A 2016;4:10801–5.
35. Esam O, Zhou G, Vasiliev A. Bridged mesoporous silsesquioxanes as potential CO_2 adsorbents. J Sol-Gel Sci Technol 2015;74:740–7.
36. Inagaki S, Guan S, Fukushima Y, Ohsuna T, Terasaki O. Novel mesoporous materials with a uniform distribution of organic groups and inorganic oxide in their frameworks. J Am Chem Soc. 1999;121:9611–4.
37. Castricum HL, Sah A, Kreiter R, Blank DHA, Vente JF, ten Elshof JE. Hydrothermally stable molecular separation membranes from organically linked silica. J Mater Chem. 2008;18:2150–8.
38. Castricum HL, Hammad F, Qureshi HF, Nijmeijer A, Winnubst L. Hybrid silica membranes with enhanced hydrogen and CO_2 separation properties. J Membr Sci 2015;488:121–8.
39. Kanezashi M, Yada K, Yoshioka T, Tsuru T. Design of silica networks for development of highly permeable hydrogen separation membranes with hydrothermal stability. J Am Chem Soc. 2009;131:414–5.
40. Li G, Kanezashi M, Tsuru T. Preparation of organic–inorganic hybrid silica membranes using organoalkoxysilanes: the effect of pendant groups. J Membr Sci 2011;379:287–95.
41. Xu R, Wang J, Kanezashi M, Yoshioka T, Tsuru T. Highly chlorine-resistant hybrid silica membranes for reverse osmosis desalination. Langmuir. 2011;27:13996–9.
42. Xu R, Kanezashi M, Yoshioka T, Okuda T, Ohshita J, Tsuru T. Tailoring the affinity of organosilica membranes by introducing polarizable ethenylene bridges and aqueous ozone modification. ACS Appl Mater Interfaces 2013;5:6147–54.
43. Xu R, Ibrahim SM, Kanezashi M, Yoshioka T, Ito K, Ohshita J, et al. New insights into the microstructure-separation properties of organosilica membranes with ethane, ethylene, and acetylene bridges. ACS Appl Mater Interfaces 2014;6:9357–64.
44. Xu R, Lin P, Zhang Q, Zhong J, Tsuru T. Development of ethenylene-bridged organosilica membranes for desalination applications. Ind Eng Chem Res. 2016;55:2183–90.
45. Chua YT, Lin CXC, Kleitz F, Zhao XZ, Smart S. Nanoporous organosilica membrane for water desalination. Chem Commun 2013;49:4534–6.
46. Agirre I, Arias PL, Castricum HL, Creatore M, Elshof JE, Paradis GG, et al. Hybrid organosilica membranes and processes: status and outlook. Sep Purif Technol 2014;121:2–12.
47. Castricum HL, Paradis GG, Mittelmeijer-Hazeleger MC, Kreiter R, Vente JF, ten Elshof JE. Tailoring the separation behavior of hybrid organosilica membranes by adjusting the structure of the organic bridging group. Adv Funct Mater 2011;21:2319–29.
48. Yamamoto K, Ohshita J, Mizumo T, Kanezashi M, Tsuru T. Preparation of hydroxyl group containing bridged organosilica membranes for water desalination. Sep Purif Technol 2015; 156:396–402.
49. Yamamoto K, Ohshita J, Mizumo T, Kanezashi M, Tsuru T. Synthesis of organically bridged trialkoxysilanes bearing acetoxymethyl groups and applications to reverse osmosis membranes. Appl Organomet Chem 2017;31:e3580.
50. Yamamoto K, Koge S, Gunji T, Ohshita J. Preparation of POSS-derived robust RO membranes for water desalination. Desalination 2017;404:322–7.
51. Yamamoto K, Koge S, Sasahara K, Mizumo T, Kaneko Y, Kanezashi M, et al. Preparation of bridged polysilsesquioxane membranes from bis [3-(triethoxysilyl) propyl] amine for water desalination. Bull Chem Soc Jpn 2017;90:1035–40.
52. Yamamoto K, Kanezashi M, Tsuru T, Ohshita J. Preparation of bridged polysilsesquioxane-based membranes containing 1, 2, 3-triazole moieties for water desalination. Polym J 2017; 49:401–6.
53. Mizumo T, Muragishi H, Yamamoto K, Ohshita J, Kanezashi M, Tsuru T. Preparation and separation properties of oxalylurea-bridged silica membranes. Appl Organo Chem 2015;29:433–8.
54. Ohshita J, Muragishi H, Yamamoto K, Mizumo T, Kanezashi M, Tsuru T. Preparation and separation properties of porous norbornane-bridged silica membrane. J Sol-Gel Sci Technol. 2015;73:365−70.
55. Yamamoto K, Muragishi H, Mizumo T, Gunji T, Kanezashi M, Tsuru T, et al. Diethylenedioxane-bridged microporous organosilica membrane for gas and water separation. Sep Purif Technol. 2018;207:370–6.
56. Zheng FT, Yamamoto K, Kanezashi M, Tsuru T, Ohshita J. Preparation of bridged silica RO membranes from copolymerization of bis(triethoxysilyl)ethene/(hydroxymethyl)triethoxysilane. Effects of ethenylene-bridge enhancing water permeability. J Membr Sci 2018;546:173–8.
57. Zheng FT, Yamamoto K, Kanezashi M, Gunji T, Tsuru T, Ohshita J. Preparation of hybrid organosilica reverse osmosis membranes by interfacial polymerization of bis[(trialkoxysilyl)propyl]amine. Chem Lett 2018;47:1210–2.

Kazuki Yamamoto is an assistant professor at Tokyo University of Science. He was born in Tokyo, Japan in 1987. He received B. Eng. degree (2010) and M. Eng. degree (2012) at Tokyo University of Since under the direction of Professor Takahiro Gunji. He was a project research fellow of Japan Science and Technology (JST) agency at Hiroshima University from 2012 to 2017. He received Ph.D. (2017) in Engineering from Hiroshima University under the direction of Professor Joji Ohshita. Since 2017, he has been in the current position at the Department of Pure and Applied Chemistry of Tokyo University of Science. His research interests are development of siloxane polymer and functional materials based on sol–gel process.

Joji Ohshita received his B. Eng. and M. Eng. degrees from Kyoto University then Dr. Eng. from Hiroshima University under the supervision of Professor Mitsuo Ishikawa in 1991. He was a research associate at Hiroshima University from 1987. During that time, he worked in the research group of Professor. Hubert Schmidbaur at the Technical University of Munich, Germany for 1 year. He was promoted to as an associate professor at Hiroshima University in 1997. After working at the Institute of Fundamental Research of Organic Chemistry, Kyushu University for 2 years from 2001, he moved back to Hiroshima University and was appointed as a professor in 2007. Currently, he is a distinguished professor at Hiroshima University. His research interest encompasses the development of functional materials grounded in element-based chemistry. He has received the Incentive Award in Synthetic Organic Chemistry, Japan (1999) and the Award of the Society of Polymer Science, Japan (2018).